Chapter 6

Conclusions and Other Evidences

This dissertation has presented a phase segregation conception for sculpting the architecture of carbon and silicon nanostructures via vapor-solid reaction growth. The salts of NaF, CaF_2, MgF_2, $CaCl_2$, $MgCl_2$, $CaBr_2$ and CaI_2 can act as self-template to assist the formation of various carbon and silicon nanostructures. The physical properties of our reactants and products are shown in Table 6.1. All of our reactions are a thermodynamically favored and highly exothermic reaction with an estimated standard enthalpy of reaction (ΔH_r^o) shown in Table 6.2.

On the basis of these results, the various morphologies of carbon and silicon materials can be purchased. For instance, the casting porous carbon can be obtained through the support of NaF to aid. In addition, the assistance of hard template-AAO has been used to cast the porous carbon into well-aligned array.

Table 6.1 The physical properties of the reactants and products.

Products	Melting point (K)	$\Delta H_f^{o}{}_{(S)}$ (kJ mol^{-1})
C (graphite)	3948	0
Si	2683	0
Na	371	0
Mg	924	0
CaC_2	2573	-60
Mg_2Si	1375	-78
$CaSi_2$	1273	-151
NaF	1269	-575
CaF_2	1676	-1226
MgF_2	1521	-1124
$CaCl_2$	1045	-796
$MgCl_2$	985	-642
$CaBr_2$	1003	-683
CaI_2	1013	-537

The core-shell CaF_2/a-C (amorphous carbon) and MgF_2/a-C nanowires can be formed while using the fluoride salts. Furthermore, the appreciated $CaCl_2$ and $MgCl_2$ can easily alter the morphology to affect the eventual product of graphite and silicon configurations. Various carbon and silicon nanostructures, such as porous carbon nanotubes, porous carbon, fibrous, lamellar, clustered nanoparticles, nanowires, coral-like, lamellar, and flake-like silicon, can be achieved. The graphitic carbon can be obtained via CaC_2 reacting with C_xCl_y. These graphite layers perform well-order arrangement at relatively low reaction temperature. The various silicon nanostructures have perfect single crystal and almost defect-free.

The results may be influenced depending on the melting point of salts. At high reaction temperature, the salts with higher melting point could be provided enough strength to support formation anisotropy core-shell nanowires like using MF_2. The wires length is tens of micrometers. In contrast, the NaF has relatively low melting point that served as self-template, so it is harder for NaF to support fabrication core-shell structure. The chloride salts cases can further confirm this explanation. The MCl_2 (M= Ca, Mg) have low melting point even lower than reaction temperature at 1023 – 1223 K. Thus, the salts are more likely to melt at this temperature interval. Due to this reason, the self-templaes can be regarded as soft template and easily alter their morphologies and dimension under fitting reaction temperatures, like 3-D porous, 2-D lamellar, 1-D fibrous, and 0-D particles. The other example is porous carbon formed via different salts NaF and $CaCl_2$ assitance. The pore shape is square-like morphology in NaF case. In contrast, by using $CaCl_2$ supplied as template, the pore shape show circle-like structure. The results have shown that the self-template having high melting point can be served as stronger template. In addition to the melting point of salts, there are other possible factors to direct the results such as reaction temperatures, composition of the products, and interfacial bonding effect.

On the other hand, further evidences are supported the phase segregation idea and the self-templates of different salts effect. These reactions were carried out by using identical experiment apparatus. Another $MgCl_2$ case, Mg metal was reacted with vapor of C_4Cl_6 at elevated temperatures 1123 – 1223 K. The prepared products are shown in Figure 6.1. The SEM image in Figure 6.1A-B shows that the sample exhibits coral-like structure at 1123 K. Increasing the reaction temperature to 1173 K, a lot of uniform particles are synthesized shown in Figure 6.1C. The TEM image (Figure 6.1D) confirms the particles which are core-shell structures. The product formed at 1223 K shows chief tubes in Figure 6.1E-F.

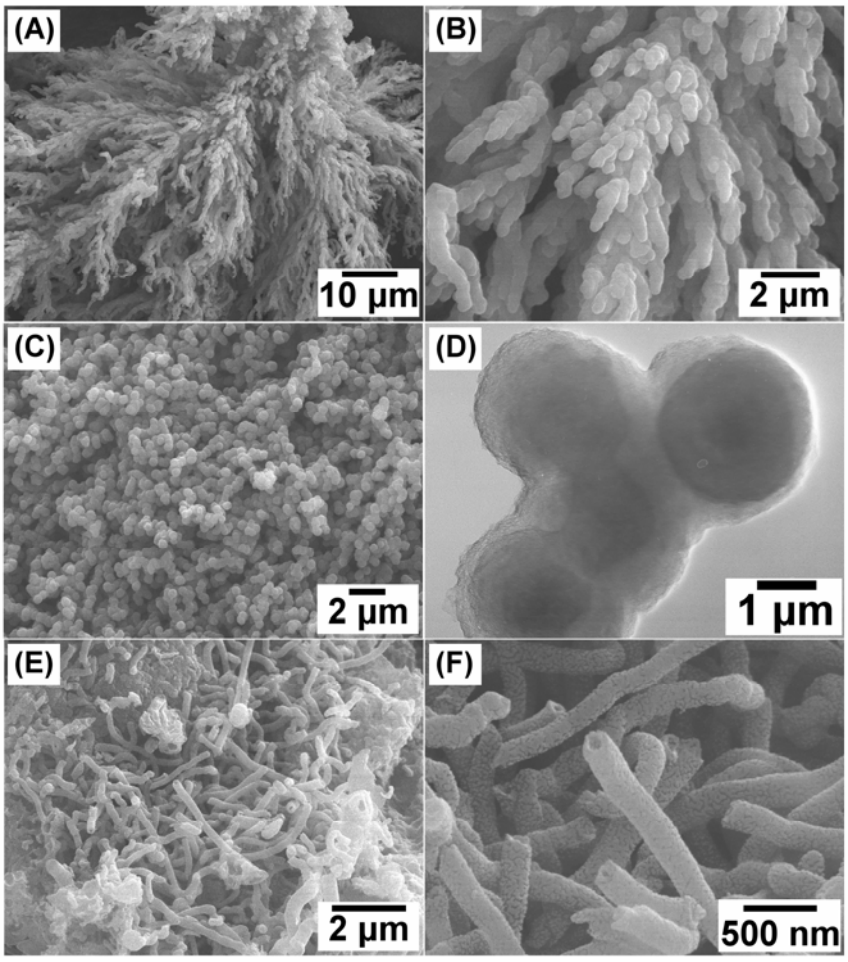

Figure 6.1 SEM images of products prepared from Mg and C_4Cl_6. (A) coral-like carbon, prepared at 1123 K; (B) core-shell structure, prepared at 1173 K; (C) carbon tubes, prepared at 1223 K.

In comparision with synthesized porous carbon materials in the atmosphere, C_6F_6 was reacted with Na at 423 K in Pyrex tube sealed under vacuum. In Figure 6.2A, a core-shell nanowire was observed. NaF crystals exist in the carbon tube, which was identified by EDX from the circled area in Figure 6.2A, shown in Figure 6.2B. The experimental data confirms the sample is NaF/*a*-C core-shell nanowire. As Figure 6.2C-D shows, SEM images of the product with removing NaF. It implies that these samples are tube structure with diameter 80 - 150 nm.

In comparison with the different halide as templates, the final products of $CaBr_2$ and CaI_2 show in Figure 6.3 and Figure 6.4. As shown in Figure 6.3, samples were prepared from CaC_2 and Br_2. The particles were observed at 1023 K, as shown in Figure 6.3A-B. The product formed at 1223 K shows mainly thin lamellar plates in Figure 6.3C-D. The similar result was performed by CaI_2 served as self-templated. The particles were obtained at 1023 K shown in Figure 6.4A-B and the thin lamellar plates were prepared shown in Figure 6.4C-D.

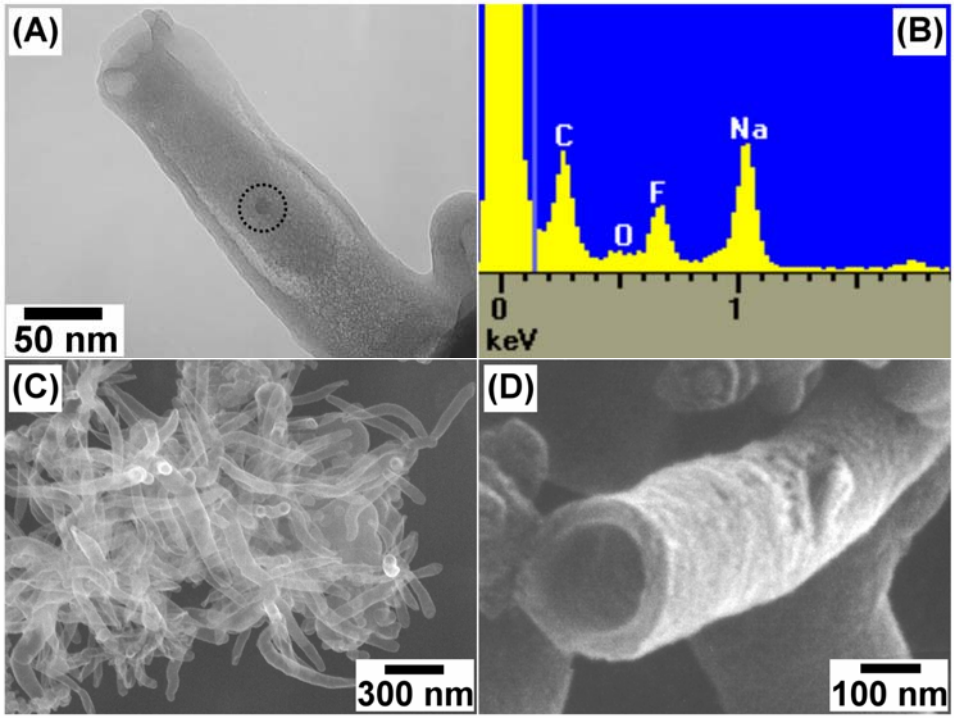

Figure 6.2 SEM and EDS Carbon/NaF nanostructures synthesized from Na and C_6F_6. (A) SEM and (B) EDS of the as-prepared product grown at 423 K; Images of carbon nanotubes after removing NaF. (C) Low and (D) high magnification SEM.

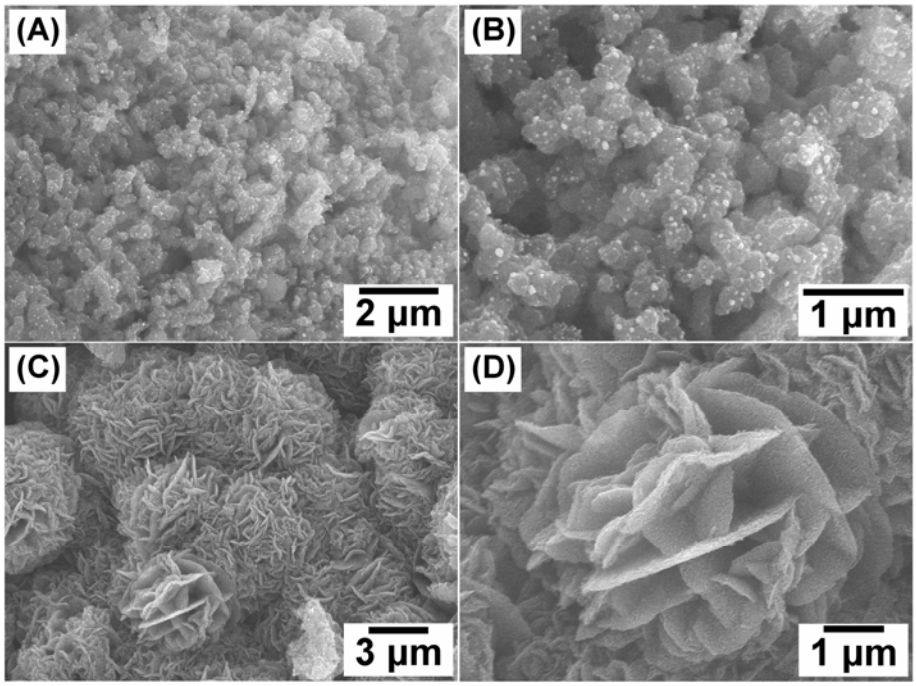

Figure 6.3 SEM images of products prepared from CaC_2 and Br_2. (A) Low and (B) high magnification carbon particles, prepared at 1023 K; (C) Low and (D) high magnification lamellar carbon, prepared at 1223 K.

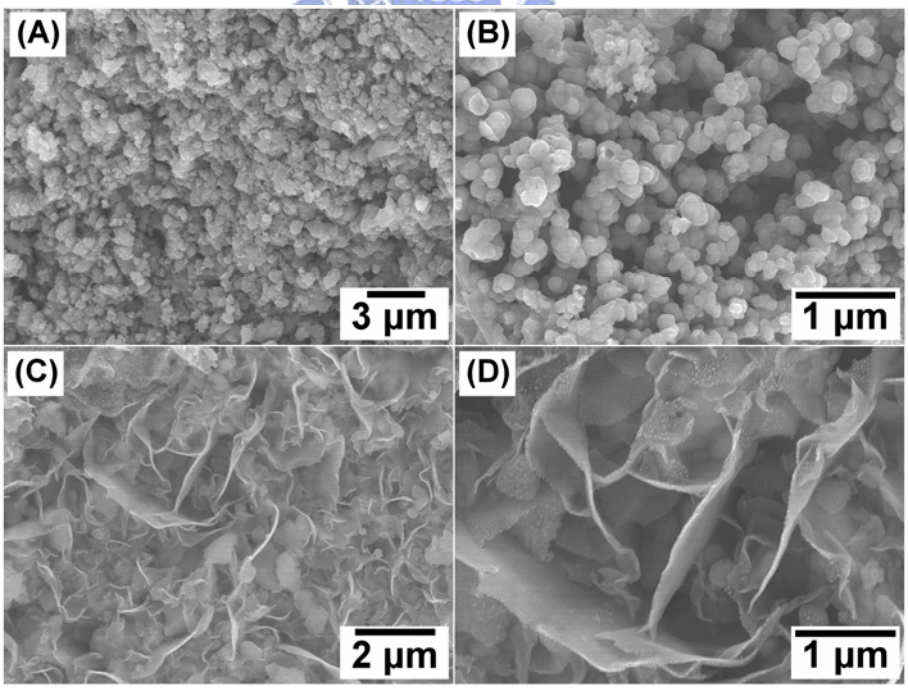

Figure 6.4 SEM images of products prepared from CaC_2 and I_2. (A) Low and (B) high magnification carbon particles, prepared at 1023 K; (C) Low and (D) high magnification lamellar carbon, prepared at 1223 K.

In conclusions, a phase segregation idea is proposed to be used to synthesize various nanostructures. To summarize our studies, Table 6.2 and Figure 6.5 give the results of the investigations. These materials are characterized carefully. The possible reaction pathways are presented to understand the mechanism of the reaction. We wish to build up a new simple and efficient route to prepare nanosized materials consisting of rich morphologies.

Table 6.2 Summary of standard enthalpy of reaction, reaction temperature and product morphologies.

Reaction	ΔH_r^o (kJ mol^{-1})	Reaction Temperature (K)	Morphologies
$3\ CaC_2 + C_6F_6 \longrightarrow 3\ CaF_2 + 12\ C$	-2543	973 – 1273	Core-shell
$3\ Mg + C_6F_6 \longrightarrow 3\ MgF_2 + 12\ C$	-1556	973 – 1273	Core-shell
$6\ Na + C_6F_6 \longrightarrow 6\ NaF + 6\ C$	-2485	323 – 673[a]	Porous
		423[b]	Tube
$2\ CaC_2 + CCl_4 \longrightarrow 2\ CaCl_2 + 5\ C$	-1377	1023	Porous
		1123	Fibrous
		1223	Lamellar
$2\ CaC_2 + C_2Cl_4 \longrightarrow 2\ CaCl_2 + 6\ C$	-1460	973	Porous
		1073	Fibrous
		1123	Lamellar
$3\ CaC_2 + C_4Cl_6 \longrightarrow 3\ CaCl_2 + 10\ C$	-2184	1023	Porous
		1123	Fibrous
		1223	Lamellar
$3\ CaC_2 + 1\ C_5Cl_6 \longrightarrow 3\ CaCl_2 + 11\ C$	-2129	1023	Porous
		1123	Fibrous
		1223	Lamellar
$2\ CaSi_2 + SiCl_4 \longrightarrow 2\ CaCl_2 + 5\ Si$	-627	1023	Porous
		1073	Wire
		1123	Coral
		1223	Lamellar
$Mg_2Si + SiCl_4 \longrightarrow 2\ MgCl_2 + 2\ Si$	-540	1023	Particle
		1073	Wire
		1123	Coral
		1223	Fake
$3\ Mg + C_4Cl_6 \longrightarrow 3\ MgCl_2 + 4\ C$	-1592	1123	Coral
		1173	Core-shell
		1223	Tube
$CaC_2 + Br_2 \longrightarrow CaBr_2 + 2\ C$	-655	1023	Particle
		1223	Lamellar
$CaC_2 + I_2 \longrightarrow CaI_2 + 2\ C$	-540	1023	Particle
		1223	Lamellar

a: atmosphere pressure.

b: low pressure.

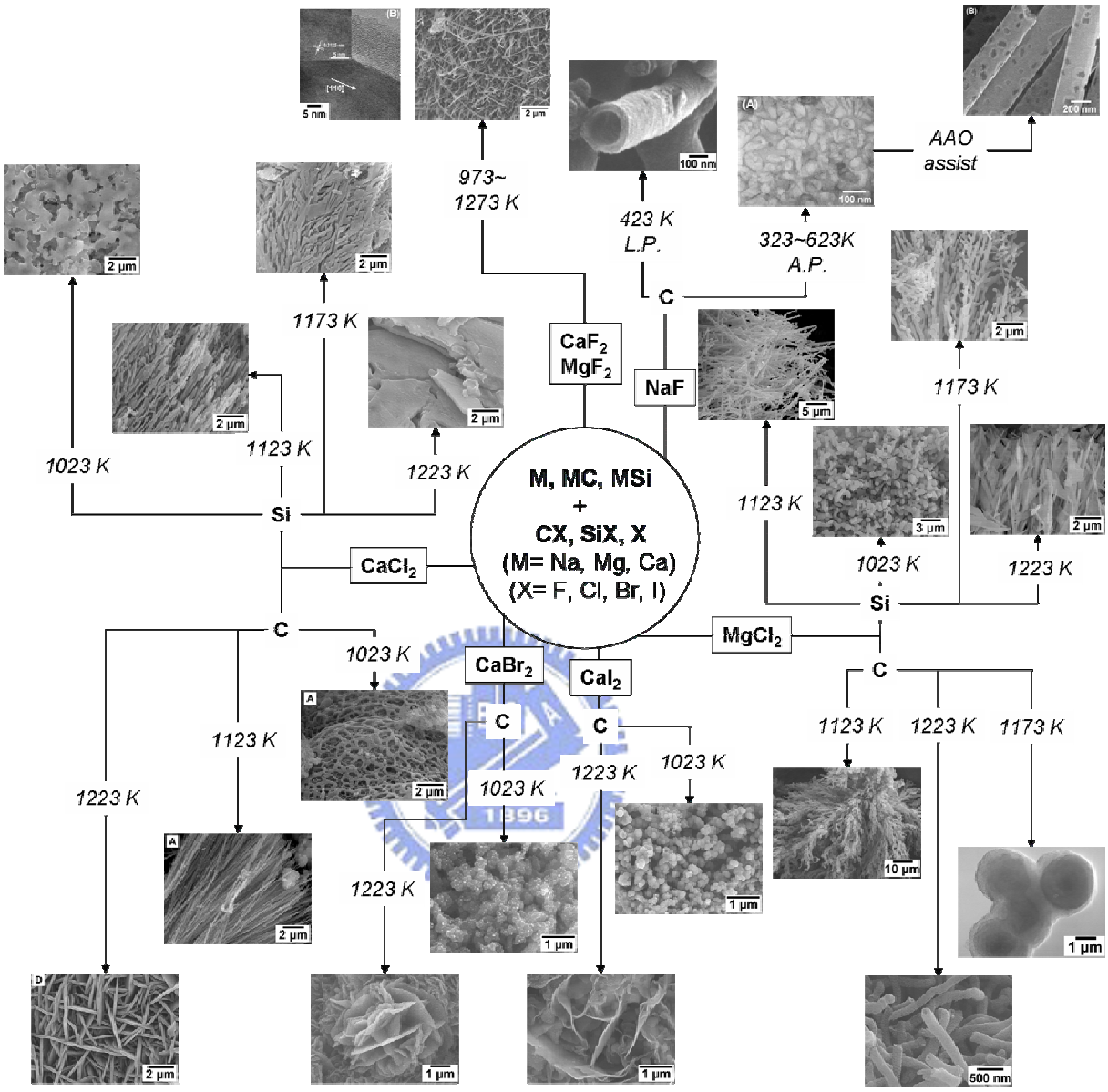

Figure 6.5 Various nanostructures synthesized sculpting by different inorganic salts assisted via vapor-solid reaction growth.